

PAPER

[View Article Online](#)
[View Journal](#) | [View Issue](#)Cite this: *Dalton Trans.*, 2020, **49**,
2989Received 22nd September 2019,
Accepted 22nd January 2020

DOI: 10.1039/c9dt03761f

rsc.li/daltonEnhancing ^{31}P NMR relaxation rates with a
kinetically inert gadolinium complex†Louise R. Tear,^{a,b} Mahon L. Maguire,^{b,c} Manuel Tropiano,^a Kezi Yao,^a
Nicola J. Farrer,^a ^a Stephen Faulkner ^a and Jurgen E. Schneider ^{b,d}

The kinetically stable heptadentate gadolinium complex Gd.pDO3A (**1.Gd**) demonstrates significant ^{31}P nuclear magnetic resonance (NMR) relaxation enhancement of biologically relevant phosphate species; adenosine triphosphate (ATP), phosphocreatine (PCr) and inorganic phosphate. Gd.pDO3A (**1.Gd**) binds these species in fast exchange, enabling the relaxation of the bulk phosphate species in solution. This gives rise to ^{31}P relaxation enhancements up to 250-fold higher than those observed for ^{31}P relaxation enhancements with the commercial MRI contrast agent Gd.DOTA (DOTAREM), **2**. Gd.pDO3A-like complexes may have potential applications as ^{31}P magnetic resonance contrast agents, since shortening the T_1 relaxation time of phosphate species would reduce the time needed to acquire ^{31}P -MR spectra.

Introduction

Lanthanide complexes are powerful tools for imaging and assay, and have played key roles in a variety of applications from contrast enhanced MRI^{1–4} to time-gated optical imaging and bioassay.^{5–7}

While the physical properties of open-shell lanthanide ions lend themselves to such applications – since the 4f electrons have little role in bonding – their chemical properties present a challenge when using lanthanides for biological applications. Lanthanide ions are too toxic to administer as free ions, form labile complexes with simple ligands, and tend to form insoluble salts with a variety of common ions. This challenge can be addressed through coordination chemistry.^{8–10} Multidentate ligands derived from macrocycles can offer high kinetic and thermodynamic stability, removing free lanthanide ions from solution, and eliminating lanthanide toxicity. Kinetic control is particularly important in this context, since precipitation of lanthanide species can act as a kinetic trap. Kinetically labile complexes can give rise to hazards in biology: for instance nephrogenic systemic fibrosis (NSF) has been cor-

related with the use of labile gadolinium complexes in clinical imaging.^{11–14}

More than thirty years after the clinical approval of the first generation of MRI contrast agents, the clinical use of MRI contrast media remains broadly focused on the use of blood pool contrast agents.¹⁵ These operate as T_1 -shortening magnetic resonance contrast agents by using the paramagnetism of gadolinium to cause rapid relaxation of water protons in bulk solution, through fast exchange between lanthanide-bound solvent and bulk solvent.^{1,16}

A variety of reports detail the preparation and use of gadolinium complexes as responsive contrast agents, where the relaxation enhancement varies depending on the interaction of the complex with an analyte of interest.⁶ However, these have found little traction in clinical applications due to difficulties in quantifying the observed response: since the contrast agent changes the behaviour of bulk water, it is very difficult to distinguish between a small quantity of complex in its “on” state (where relaxation is enhanced greatly) and a large quantity of complex in the “off” state. This dichotomy has been successfully addressed in the case of luminescent complexes, where ratiometric imaging methods can be used to quantify behaviour on the basis of taking the ratio between two different emission wavelengths.^{7,17} However, such an approach is very challenging in the context of MRI, though Caravan and co-workers have had some success in quantitative imaging using the DREMR protocol, which measures relaxation at two different fields and relies on differences in field dependence of relaxivity between the “off” and “on” forms of a complex.¹⁸

In this manuscript, we describe how ^{31}P NMR methods can be used to probe the interaction of a lanthanide complex with some ionic phosphate species.^{6,19–21} Relatively weak and

^aChemistry Research Laboratory, University of Oxford, Mansfield Road, OX1 3TA, UK. E-mail: stephen.faulkner@chem.ox.ac.uk; Tel: +44 (0)1865 272640

^bBritish Heart Foundation Experimental MR Unit (BMRU), University of Oxford, Roosevelt Drive, Oxford, OX3 7BN, UK

^cCentre for Preclinical Imaging, University of Liverpool, Nuffield Wing, Sherrington Building, Crown Street, Liverpool, L69 3BX, UK

^dLeeds Institute of Cardiovascular and Metabolic Medicine, Biomedical Imaging Science Department, University of Leeds, Clarendon Way, Leeds, LS2 9JT, UK

†Electronic supplementary information (ESI) available: Materials and methods including spectroscopy, determination of binding constants and isotherms. See DOI: 10.1039/c9dt03761f

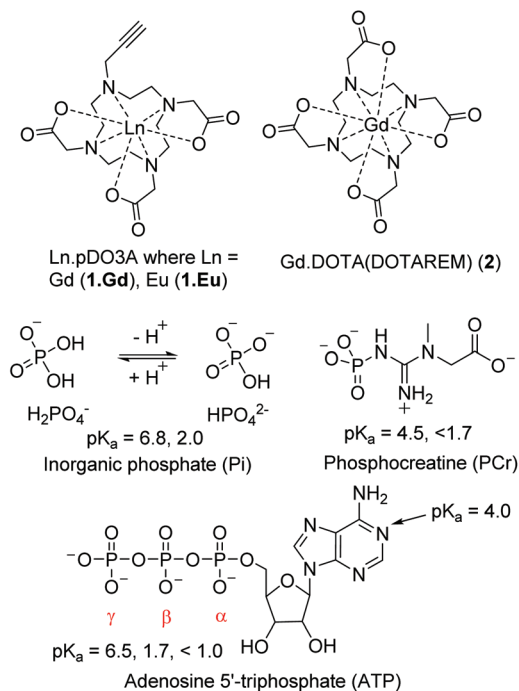


Fig. 1 Structures of complexes discussed in this study; commercial contrast agent Gd.DOTA; complexes of pDO3A complexes of Gd (**1.Gd**) and Eu (**1.Eu**) which are investigated in this study; relevant phosphate species with reported pK_a values (H_2O) of the phosphate groups.^{27–29}

rapidly reversible phosphate binding gives rise to ^{31}P relaxation enhancement for bulk phosphate species, while different species respond to the complex to different degrees. Such results potentially open up a new strategy for imaging.

Here we report our investigation into using the kinetically inert lanthanide complex (Gd.pDO3A (**1.Gd**) Fig. 1)^{22–26} as a ^{31}P contrast agent for enhancing phosphorus relaxation. **1.Gd** comes from a family of pDO3A complexes which we have previously used as building blocks for more complex architectures: it combines high kinetic stability with charge neutrality: we reasoned that this combination would reduce the affinity for phosphate, permitting us to anticipate relatively rapid exchange of bound phosphate with bulk. As such we chose this system to test the hypothesis of using **1.Gd** as a contrast medium for ^{31}P relaxation enhancement.

Results and discussion

Both gadolinium (**1.Gd**) and europium (**1.Eu**) pDO3A complexes were synthesized and characterised using established procedures.²² Given the importance of maintaining the integrity of these complexes and the issues associated with the formation of phosphate colloids with free lanthanide ions,^{11–14} we resolved to explore their stability before embarking on a more detailed study. In such a system, precipitation constitutes a kinetic trap, and absolute measurements of thermodynamic stability can be misleading as they do not guarantee

safety of complexes where the system is under thermodynamic control.¹¹ Under such circumstances, kinetic stability is essential, and our previous studies on heterometallic systems²⁶ led us to believe that these systems would be kinetically inert. The method of Tóth³⁰ was used to explore the stability of the complexes by challenging the europium complex with an excess of free gadolinium ions in aqueous solution. No change in the form of the observed spectrum was observed over a period of five days, indicating that the complex is kinetically inert (since the luminescence spectra of free and complexed europium are very different, as can be seen in the ESI† to this paper).

The interaction of **1.Eu** with three phosphate metabolites – inorganic phosphate (P_i), PCr and ATP – was assessed by luminescence spectroscopy. Titration of each metabolite with **1.Eu** in HEPES buffer at pH 7.4 resulted in modulation of the Eu emission intensity. Changes to the emission spectra clearly reveal a change to the local coordination environment at the metal centre (Fig. 2, and Fig. S1 and S2†), from which it is possible to infer phosphate displacing water at the metal centre. In the case of inorganic phosphate (Fig. 2), the consequences of binding are clear, with significant changes to the local ligand field being evident from changes to the fine structure of the $^5\text{D}_0\text{--}^7\text{F}_1$ transition (around 595 nm) and to the relative intensity of the $^5\text{D}_0\text{--}^7\text{F}_2$ transition, which is hypersensitive to local symmetry.

The integrated intensity of the $^5\text{D}_0\text{--}^7\text{F}_2$ transition ($\lambda_{\text{em}} = 617 \text{ nm}$) was plotted against the phosphate species concentration to determine the strength of the binding interaction (the inset to Fig. 2 shows a binding isotherm for inorganic phosphate: the others are recorded in Fig. S1 and S2†).

These were fitted using Dynafit^{®31} and modelled to a 1 : 1 binding equilibrium (ESI, eqn (S1)†) to determine the association constants K_a listed in Table 1. Since the values calculated were measured in the presence of HEPES, which has limited

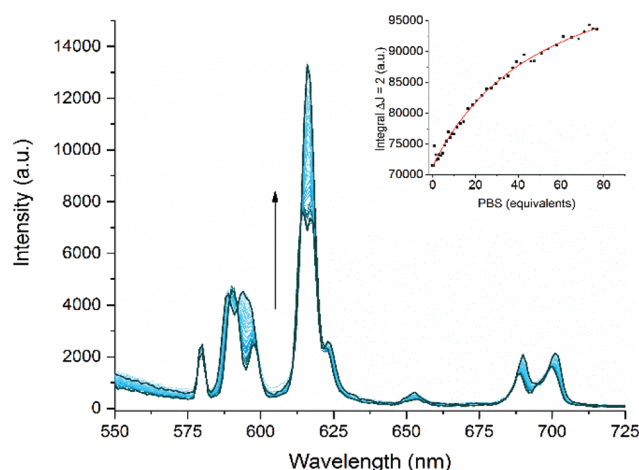


Fig. 2 Main figure: changes to the total emission spectrum ($\lambda_{\text{ex}} = 394 \text{ nm}$) of a solution of **1.Eu** in HEPES buffer with increasing concentration of inorganic phosphate. Inset: the binding isotherm obtained from changes in the intensity of the $^5\text{D}_0\text{--}^7\text{F}_2$ emission band centred on 617 nm and fitted using Dynafit[®].³¹



Table 1 Association constants (K_a) for **1.Eu** with each phosphate species, pH 7.4, $\lambda_{\text{ex}} = 394$ nm

Phosphate species ^a	K_a ^b (M^{-1})	95% confidence interval
P_i ^c	194 ± 12	[172–218]
ATP	200 ± 8	[185–216]
PCr	120 ± 8	[104–138]

^a All samples in 10 mM HEPES, with 0.1 mM **1.Eu**. ^b \pm standard deviation. ^c In the absence of HEPES an apparent K_a of 261 ± 15 [232–292] was determined.

ionic strength and can potentially interact with lanthanide complexes, these values represent effective binding constants, but clearly reveal consistent binding of a variety of phosphate species, with slightly weaker binding of PCr as a result of its zwitterionic nature.

The observed values of K_a are fully consistent with fast exchange between bulk phosphate and phosphate bound to **1.Eu**. The three phosphate species all exhibit very similar affinity constants. Binding of phosphate was further demonstrated by measuring the luminescence lifetimes in H_2O and D_2O , and determining the number of inner-sphere water molecules using the modified Horrocks equation.³² This revealed that $q = 2$ for **1.Eu** in the absence of phosphate, but $q = 0.9$ in the presence of phosphate – consistent with monodentate coordination of phosphate in line with literature precedent.⁶

To further explore exchange, we used **1.Gd** to explore the possibility of observing changes to the bulk relaxation rates of phosphate species in the presence of increasing concentrations of **1.Gd**, reasoning that fast exchange would lead to clear concentration dependent enhancement of the ^{31}P longitudinal relaxation rates, in the same way that conventional MRI contrast agents enhance the relaxation of bulk water. ^{31}P relaxation rates ($R_1 = 1/T_1$) were measured for ATP, PCr and P_i with increasing concentrations of **1.Gd** (Fig. 3).

1.Gd showed a significant linear relaxation enhancement of all phosphate species (Fig. 3), suggesting that fast exchange is

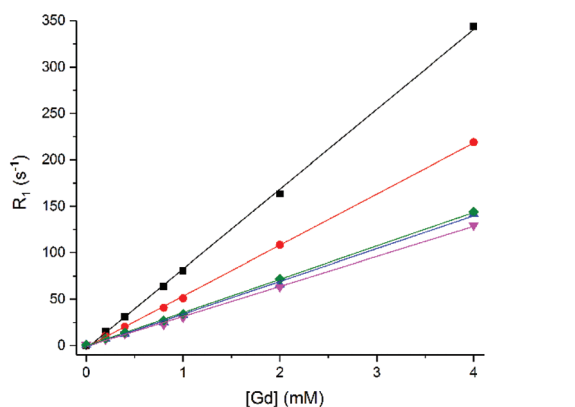


Fig. 3 ^{31}P Relaxation rate (R_1) of P_i (■), PCr (●) and α -ATP (▼), β -ATP (◆), γ -ATP (▲) (8.7, 5.5 and 7.9 mM) versus concentration of **1.Gd**, pH 7.2, 162 MHz, 298 K.

indeed occurring. This linear enhancement also confirms that the gadolinium complex is kinetically stable under the conditions of the experiment, since exchange of gadolinium and formation of a new gadolinium bound species results in significant curvature to the plot, as previously observed by Muller and co-workers (who observed significant competition between ATP and gadolinium complexes of DTPA bis amide ligands).³³

The relaxivities obtained ($r_1 = 1/([\text{Gd}]T_1)$) are displayed in Table 2 for **1.Gd**. The table also shows the ^{31}P relaxivity properties for **2** (Gd.DOTA, Dotarem®) for comparison. These values for **1.Gd** are all greater than $30 \text{ mM}^{-1} \text{ s}^{-1}$, with the most significant effect observed for P_i followed by PCr and then ATP. This is most likely to be a result of the size of the phosphate molecule and the consequently easy access to the Gd binding site.

Increasing concentrations of contrast agent **2** resulted in a much smaller, though still linear, relaxation enhancement across all five phosphate resonances (P_i , PCr, α -ATP, β -ATP, γ -ATP) (Table 2 and Fig S4†). The ^{31}P relaxivity values ($r_1 = 1/([\text{Gd}]T_1)$) of all phosphate species were below $0.5 \text{ mM}^{-1} \text{ s}^{-1}$. These relaxivity values for **2** are more than 60 times smaller than the relaxivity values measured for **1.Gd**.

Taking the observations on **1.Gd** together with those on **2**, it is clear that phosphate affinity is playing an important role in relaxation rate enhancement. For **2**, which displays negligible affinity for phosphate, the small enhancements observed are likely to be the consequence of an outer sphere interaction.

Outer-sphere relaxation is defined by diffusion, the distance of closest approach and the electronic relaxation time of the metal ion.³⁴ For complexes of a similar size and molecular weight, the outer-sphere contribution to longitudinal relaxation rate is considered to be comparable and independent of differences in functional groups on the ligand. On this basis, we can use the relaxivity measurements obtained using **2** to estimate the inner sphere contribution to ^{31}P relaxivity with **1.Gd**, using eqn (1).

$$r_1 = r_1^{\text{IS}} + r_1^{\text{OS}} \quad (1)$$

From this equation the inner-sphere contribution to the overall observed ^{31}P relaxivity for **1.Gd** is estimated to be $\geq 99\%$ and is clearly the dominant effect. This is much greater than is

Table 2 ^{31}P relaxivity (r_1) of phosphate species with **1.Gd** and **2**, 162 MHz, pH 7.2, 298 K

Phosphate species ^a	r_1 ^b ($\text{mM Gd}^{-1} \text{ s}^{-1}$)	
	1.Gd	2
P_i	85.96 ± 1.00	0.35 ± 0.01
PCr	54.97 ± 0.48	0.24 ± 0.01
α -ATP	32.35 ± 0.46	0.39 ± 0.03
β -ATP	35.97 ± 0.35	0.27 ± 0.01
γ -ATP	35.30 ± 0.64	0.25 ± 0.01

^a Solution contains [PBS] = 8.7 mM, [PCr] = 5.5 mM, [ATP] = 7.9 mM. ^b \pm Standard error of linear fit, R^2 values >0.99 for all fits.



commonly observed for ^1H relaxivity, where the outer sphere contribution for a $q = 1$ complex can be around 40% (at imaging field strengths).^{35,36} The much lower outer-sphere contribution for phosphates undoubtedly reflects that there are invariably many water molecules in the outer coordination sphere of a complex. Since the total concentration of phosphate nuclei will be around three orders of magnitude lower than that of water protons (25 mM total phosphate species *versus* ~55 M water) the contribution of second-sphere phosphate molecules is always likely to be relatively small.

Since phosphate binds to **1.Gd**, it was anticipated that phosphate binding would exclude water from the inner coordination sphere. To confirm this, the ^1H water relaxation rate was measured with increasing concentrations of **1.Gd** in distilled water and in phosphate solution (Fig. 4, values in Table 3). The relaxivity in water is very similar to that for DO3A³⁷ and greater than that for Dotarem, as would be expected for a complex with $q = 2$.¹

The ^1H relaxivity was found to be about 16% lower in phosphate solution than in distilled water. This is due to the competition between water and phosphate species for the gadolinium centre, which reduces the concentration of bound water molecules relative to bulk. This suggests that a combination of the decrease in ^1H signal and increase in ^{31}P signal may allow the possibility for ratiometric determination of phosphate from multinuclear relaxometric measurements – though it is clear that current instrumentation would make such simultaneous dual measurements extremely challenging.

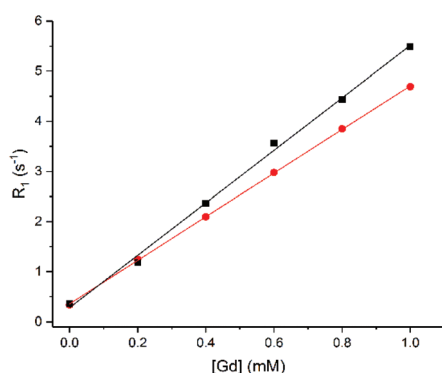


Fig. 4 ^1H water relaxation rate (R_1) in DI water (■) or phosphate solution (●) (8.7 mM PBS, 5.5 mM PCr and 7.9 mM ATP) *versus* concentration of **1.Gd**, pH 7.2, 400 MHz, 298 K. Error bars are within the size of the data points.

Table 3 H_2O ^1H relaxivity (r_1) with **1.Gd** at 400 MHz, pH 7.2, 298 K

Complex	r_1^b (mM $\text{Gd}^{-1} \text{s}^{-1}$)	
	Water	Phosphate solution ^a
1.Gd	5.24 ± 0.13	4.36 ± 0.02

^a Phosphate solution = [PBS] = 8.7 mM, [PCr] = 5.5 mM, [ATP] = 7.9 mM. ^b \pm Standard error of linear fit, R^2 values >0.99 for all fits.

Experimental

For materials, methods and procedures see ESI.†

Conclusions

In this study, we have shown how binding and fast exchange between a gadolinium complex and anionic phosphate species can be exploited to enhance relaxation of bulk phosphate anions in solution. We have demonstrated significant ^{31}P relaxation enhancement using a kinetically inert heptadentate lanthanide complex **1.Gd**. We observe dramatic enhancements in relaxation for a variety of phosphorus containing species (particularly phosphate itself, ATP and phosphocreatine). Preliminary studies suggest that this **1.Gd** is not internalised by cells to any significant extent,³⁸ limiting the biological application of this complex to extracellular investigation without further derivation. The use of phosphate contrast media may prove a profitable avenue for investigation if these issues of cellular uptake can be addressed.

Conflicts of interest

There are no conflicts to declare.

Acknowledgements

This work was supported by funding from the Engineering and Physical Sciences Research Council (EPSRC), the Medical Research Council (MRC) [grant number EP/L016052/1] and the British Heart Foundation (FS/11/50/29038). NF thanks the Wellcome Trust (201406/Z/16/Z), Cancer Research UK (C5255/A18085) through the Cancer Research UK Oxford Centre, L'Oréal (Women in Science Fellowship) and Singapore Chemical Group (Innovation Fund Young Researcher Award) for funding.

Notes and references

- P. Caravan, J. J. Ellison, T. J. McMurphy and R. B. Lauffer, *Chem. Rev.*, 1999, **99**, 2293.
- J. Lohrke, T. Frenzel, J. Endrikat, F. C. Alves, T. M. Grist, M. Law, J. M. Lee, T. Leiner, K. C. Li, K. Nikolaou, M. R. Prince, H. H. Schild, J. C. Weinreb, K. Yoshikawa and H. Pietsch, *Adv. Ther.*, 2016, **33**, 1.
- L. M. De León-Rodríguez, A. F. Martins, M. C. Pinho, N. M. Rofsky and A. D. Sherry, *J. Magn. Reson. Imaging*, 2015, **42**, 545.
- G.-P. Yan, L. Robinson and P. Hogg, *Radiography*, 2007, **13**, e5.
- K. Y. Zhang, Q. Yu, H. Wei, S. Liu, Q. Zhao and W. Huang, *Chem. Rev.*, 2018, **118**, 1770.
- S. J. Butler and D. Parker, *Chem. Soc. Rev.*, 2013, **42**, 1652.
- S. H. Hewitt and S. J. Butler, *Chem. Commun.*, 2018, **54**, 6635.



- 8 T. J. Sørensen and S. Faulkner, *Acc. Chem. Res.*, 2018, **51**, 2493.
- 9 D. Messeri, M. P. Lowe, D. Parker and M. Botta, *Chem. Commun.*, 2001, **1**, 2742.
- 10 M. Tropicano, O. A. Blackburn, J. A. Tilney, L. R. Hill, M. P. Placidi, R. J. Aarons, D. Sykes, M. W. Jones, A. M. Kenwright, J. S. Snaith, T. J. Sørensen and S. Faulkner, *Chem. – Eur. J.*, 2013, **19**, 16566.
- 11 M. Le Fur and P. Caravan, *Metallomics*, 2019, **11**, 240.
- 12 W. A. High, R. A. Ayers, J. Chandler, G. Zito and S. E. Cowper, *J. Am. Acad. Dermatol.*, 2007, **56**, 21.
- 13 P. Marckmann, L. Skov, K. Rossen, A. Dupont, M. B. Damholt, J. G. Heaf and H. S. Thomsen, *J. Am. Soc. Nephrol.*, 2006, **17**, 2359.
- 14 T. Grobner, *Nephrol., Dial., Transplant.*, 2006, **21**, 1104.
- 15 J. Wahsner, E. M. Gale, A. Rodríguez-Rodríguez and P. Caravan, *Chem. Rev.*, 2019, **119**, 957.
- 16 V. C. Pierre, M. J. Allen and P. Caravan, *J. Biol. Inorg. Chem.*, 2014, **19**, 127–131.
- 17 T. J. Sørensen, A. M. Kenwright and S. Faulkner, *Chem. Sci.*, 2015, **6**, 2054.
- 18 J. K. Alford, A. G. Sorensen, T. Benner, B. A. Chronik, W. B. Handler, T. J. Scholl, G. Madan and P. Caravan, *Proc. Int. Soc. Magn. Reson. Med.*, 2011, **19**, 452.
- 19 P. Atkinson, Y. Bretonnière, D. Parker and G. Muller, *Helv. Chim. Acta*, 2005, **88**, 391.
- 20 J. I. Bruce, R. S. Dickins, L. J. Govenlock, T. Gunnlaugsson, S. Lopinski, M. P. Lowe, D. Parker, R. D. Peacock, J. J. B. Perry, S. Aime and M. Botta, *J. Am. Chem. Soc.*, 2000, **122**, 9674.
- 21 R. N. Muller, B. Radüchel, S. Laurent, J. Platzek, C. Piérart, P. Mareski and L. Vander Elst, *Eur. J. Inorg. Chem.*, 1999, 1949.
- 22 M. Jauregui, W. S. Perry, C. Allain, L. R. Vidler, M. C. Willis, A. M. Kenwright, J. S. Snaith, G. J. Stasiuk, M. P. Lowe and S. Faulkner, *Dalton Trans.*, 2009, 6283.
- 23 A. K. R. Junker, M. Tropicano, S. Faulkner, T. J. Sørensen, A. Kathrine, R. Junker, M. Tropicano, S. Faulkner and T. Just Sørensen, *Inorg. Chem.*, 2016, **55**, 12299.
- 24 M. Tropicano, N. L. Kilah, M. Morten, H. Rahman, J. J. Davis, P. D. Beer and S. Faulkner, *J. Am. Chem. Soc.*, 2011, **133**, 11847.
- 25 C. Allain, P. D. Beer, S. Faulkner, M. W. Jones, A. M. Kenwright, N. L. Kilah, R. C. Knighton, T. J. Sørensen and M. Tropicano, *Chem. Sci.*, 2013, **4**, 489.
- 26 M. Tropicano, A. M. Kenwright and S. Faulkner, *Chem. – Eur. J.*, 2015, **21**, 5697.
- 27 P. Oesper, in *Phosphorus Metabolism*, ed. W. D. McElroy and B. Glass, John Hopkins University Press, Baltimore, 1951, vol. I, pp. 523–536.
- 28 L. Chen, *Biomed. Res.*, 2017, **28**, 8195.
- 29 P. Kaczmarek, W. Szczepanik and M. Jezowska-Bojczuk, *Dalton Trans.*, 2005, 3653.
- 30 É. Tóth, R. Király, J. Platzek, B. Radüchel and E. Brücher, *Inorg. Chim. Acta*, 1996, **249**, 191.
- 31 P. Kuzmič, *Methods Enzymol.*, 2009, **467**, 247.
- 32 A. Beeby, I. M. Clarkson, R. S. Dickins, S. Faulkner, D. Parker, L. Royle, A. S. de Sousa, J. A. G. Williams and M. Woods, *J. Chem. Soc., Perkin Trans. 2*, 1999, 493.
- 33 L. Vander Elst, Y. Van Haverbeke, J. F. Goudemant and R. N. Muller, *Magn. Reson. Med.*, 1994, **31**, 437.
- 34 S. Aime, M. Botta, M. Fasano and E. Terreno, *Chem. Soc. Rev.*, 1998, **27**, 19.
- 35 S. Aime, A. S. Batsanov, M. Botta, J. A. K. Howard, D. Parker, K. Senanayake and G. Williams, *Inorg. Chem.*, 1994, **33**, 4696.
- 36 M. Botta, *Eur. J. Inorg. Chem.*, 2000, 399.
- 37 P. Placidi, L. S. Natrajan, D. Sykes, A. M. Kenwright and S. Faulkner, *Helv. Chim. Acta*, 2009, **92**, 2427.
- 38 L. R. Tear, *Molecular Imaging Probes for ³¹P Contrast*, DPhil Thesis, University of Oxford, Oxford, UK, 2018.

